

# Disentangling the ligand and electronic structure in $\text{KVPO}_4\text{F}_{1-x}\text{O}_x$ positive electrode materials by Valence-to-Core X-ray emission spectroscopy

Jazer Jose H. Togonon<sup>1,2,3</sup>, Antonella Iadecola<sup>4,5,\*</sup>, Romain Wernert<sup>2,4,6</sup>, Kriti Choudhary<sup>3,4,7</sup>,  
Mauro Rovezzi<sup>8</sup>, Jean-Noël Chotard<sup>3,4,7</sup>, Lorenzo Stievano<sup>3,4,6</sup>,  
Alessandro Longo<sup>9,10,\*</sup>, Laurence Croguennec<sup>2,3,4,\*</sup>

## Authors' Address

<sup>1</sup> Synchrotron SOLEIL, L'Orme des Merisiers, Saint-Aubin, 91192 Gif-sur-Yvette, France

<sup>2</sup> Univ. Bordeaux, CNRS, Bordeaux INP, ICMCB, UMR 5026, F-33600 Pessac, France

<sup>3</sup> ALISTORE-ERI European Research Institute, FR CNRS 3104, F-80039 Amiens Cedex 1, France

<sup>4</sup> RS2E, Réseau Français sur le Stockage Electrochimique de l'Energie, FR CNRS #3459, Amiens F-80039 Cedex 1, France

<sup>5</sup> Physicochimie des Electrolytes, Nanosystèmes Interfaciaux (PHENIX), Sorbonne Université, CNRS, 75252 Paris, France

<sup>6</sup> ICGM, Univ. Montpellier, CNRS, ENSCM, 34095 Montpellier, France

<sup>7</sup> Université de Picardie Jules Verne, Laboratoire de Réactivité et Chimie des Solides (LRCS), 15 rue Baudelocque, 80000, Amiens, France

<sup>8</sup> Univ. Grenoble Alpes, CNRS, IRD, Irstea, Météo France, OSUG, FAME, F-38000 Grenoble, France

<sup>9</sup> European Synchrotron Radiation Facility (ESRF), 71, Avenue des Martyrs, Grenoble F-38000, France

<sup>10</sup> Istituto per lo Studio dei Materiali Nanostrutturati (ISMN)-CNR, UOS Palermo, via Ugo La Malfa 153, Palermo 90146, Italy

\*Corresponding authors: [antonella.iadecola@synchrotron-soleil.fr](mailto:antonella.iadecola@synchrotron-soleil.fr); [alessandro.longo@esrf.fr](mailto:alessandro.longo@esrf.fr),  
[laurence.croguennec@icmcb.cnrs.fr](mailto:laurence.croguennec@icmcb.cnrs.fr)

**Keywords:** Valence-to-Core X-ray emission spectroscopy, electronic structure, vanadium fluoride phosphate, vanadium oxide phosphate, vanadyl-type bond, potassium-ion battery, X-ray emission spectroscopy

## Supplementary Information

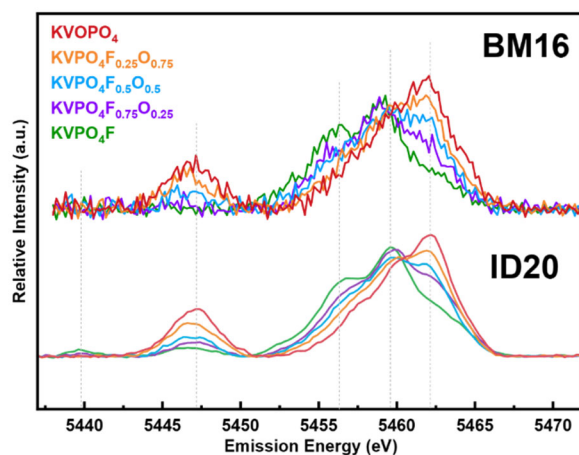
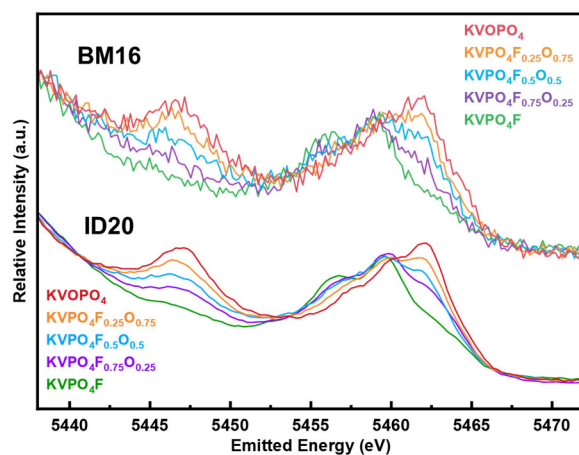


Figure S1. Vanadium VtC XES spectra from BM16 and ID20 at the European Synchrotron and Radiation Facility (ESRF) showing reproducibility of the results from the measurements performed. Raw spectra obtained (top) and baseline-subtracted spectra (bottom)

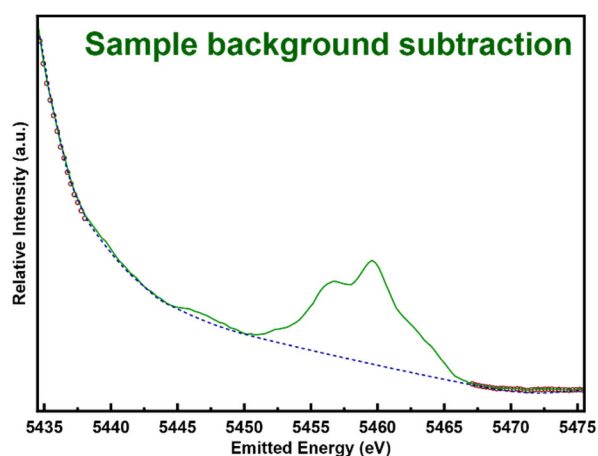


Figure S2. VtC data background subtraction<sup>1</sup>

*Table S1. KVPO<sub>4</sub>F input file for the FDMNES calculation*

```
! FDMNES indata file
! Calculation for the V VtC_Kbeta KVPO4F
! Finite difference method calculation with convolution

Filout
  pristine_cell/pristine_vfp/pristine_vfp

Range      ! Energy range of calculation (eV)
-40. 0.2 -10 0.1 -5 0.05 0. 0.1 5 0.2 10. .5 40. 1 60. ! first energy, step, intermediary
energy, step ..., last energy

Radius     ! Radius of the cluster where final state calculation is performed
8.0

SCF        ! Activation of the self consistent field calculation

Green      ! Inclusion of the green function

Density_all ! Densities of state results

Edge
K

XES

Z_absorber
23

Spgroup
33

Occupancy

Crystal_t
  12.8223 6.39721 10.6203 90 90 90 ! Cell parameters
!Atoms
19 0.3802 0.7788 0.3018 1.02      !Potassium
19 0.1044 0.6972 0.0590 0.97
23 0.3854 0.4967 0          1.00      !Vanadium
23 0.2469 0.2514 0.2469 1.00
15 0.4988 0.3311 0.2501 1.00      !Phosphorus
15 0.1817 0.4991 0.4991 1.00
8  0.4848 0.4865 0.1406 1.00      !Oxygen
8  0.5122 0.4682 0.3691 1.00
8  0.4008 0.1959 0.2689 1.00
8  0.5955 0.1935 0.2286 1.00
8  0.1112 0.3107 0.5292 1.00
8  0.1127 0.6910 0.4722 1.00
8  0.2501 0.5377 0.6163 1.00
8  0.2566 0.4580 0.3888 1.00
9  0.2706 0.5230 0.8788 1.00      !Fluorine
9  0.2716 0.4777 0.1266 1.00

!!!Convolution keyword : broadening with a width increasing versus energy as an arctangent

Estart
-20

Efermi
-5.0

Convolution
42 11 10

Gamma_hole
0.7

Gaussian
1.0

End
```

Table S2. KVOPO<sub>4</sub> input file for the FDMNES calculation

```

! FDMNES indata file
! Calculation for the V VtC_Kbeta KVOPO4
! Finite difference method calculation with convolution

Filout
  pristine_cell/pristine_vop/pristine_vop

Range      ! Energy range of calculation (eV)
-40. 0.2 -10 0.1 -5 0.05 0. 0.1 5 0.2 10. .5 40. 1 60. ! first energy, step, intermediary
energy, step ..., last energy

Radius     ! Radius of the cluster where final state calculation is performed
8.0

SCF        ! Activation of the self consistent field calculation

Green      ! Inclusion of the green function

Density_all ! Densities of state results

Edge
K

XES

Z_absorber
23

Spgroup
33

Occupancy

Crystal_t
12.7618 6.3654 10.5126 90 90 90 !Cell parameters
!Atoms
19 0.3820 0.3820 0.7827 1.04 !Potassium
19 0.1030 0.7047 0.0596 0.96
23 0.3765 0.4960 0 1.00 !Vanadium
23 0.2478 0.2739 0.2390 1.00
15 0.4961 0.3307 0.2490 1.00 !Phosphorus
15 0.1805 0.4980 0.5052 1.00
8 0.4830 0.4820 0.1360 1.00 !Oxygen
8 0.5120 0.4680 0.3680 1.00
8 0.3995 0.1910 0.2720 1.00
8 0.5936 0.1900 0.2330 1.00
8 0.1100 0.3060 0.5290 1.00
8 0.1090 0.6860 0.4740 1.00
8 0.2500 0.5370 0.6210 1.00
8 0.2570 0.4590 0.3940 1.00
8 0.2870 0.5280 0.8820 1.00 !Oxygen vanadyl oxygen
8 0.2680 0.4630 0.1320 1.00

!!!Convolution keyword : broadening with a width increasing versus energy as an arctangent

Estart
-20

Efermi
-5.0

Convolution
42 11 10

Gamma_hole
0.7

Gaussian
1.0

End

```

Table S3. Calculated bond valence sum (BVS) for all pristine and reference materials. <sup>2</sup>

	$V_{cis}$	$V_{trans}$	$V_{average}$
<b>KVPO<sub>4</sub>F</b>	3.10	2.96	<b>3.03</b>
<b>KVPO<sub>4</sub>F<sub>0.75</sub>O<sub>0.25</sub></b>	3.33	3.18	<b>3.25</b>
<b>KVPO<sub>4</sub>F<sub>0.5</sub>O<sub>0.5</sub></b>	3.57	3.43	<b>3.50</b>
<b>KVPO<sub>4</sub>F<sub>0.25</sub>O<sub>0.75</sub></b>	3.85	3.62	<b>3.74</b>
<b>KVOPO<sub>4</sub></b>	4.05	3.86	<b>3.96</b>
<b>Na<sub>3</sub>V<sub>2</sub>(PO<sub>4</sub>)<sub>3</sub></b>			<b>3.07</b>
<b>Na<sub>1</sub>V<sub>2</sub>(PO<sub>4</sub>)<sub>3</sub></b>			<b>4.05</b>
<b>NaVOPO<sub>4</sub></b>			<b>3.90</b>
<b>β-VOPO<sub>4</sub></b>			<b>5.26</b>

<b>Bonding</b>	$R_o$	$b$
<b>V<sup>III</sup>-O<sup>(-2)</sup></b>	1.743	
<b>V<sup>III</sup>-F<sup>(-1)</sup></b>	1.702	
<b>V<sup>IV</sup>-O<sup>(-2)</sup></b>	1.784	0.37
<b>V<sup>IV</sup>=O<sup>(-2)</sup></b>	1.735	
<b>V<sup>IV</sup>-F<sup>(-1)</sup></b>	1.700	
<b>V<sup>V</sup>-O<sup>(-2)</sup></b>	1.803	

$$BVS = \sum_{R_{exp}=1}^6 e^{\frac{R_o - R_{exp}}{b}}$$

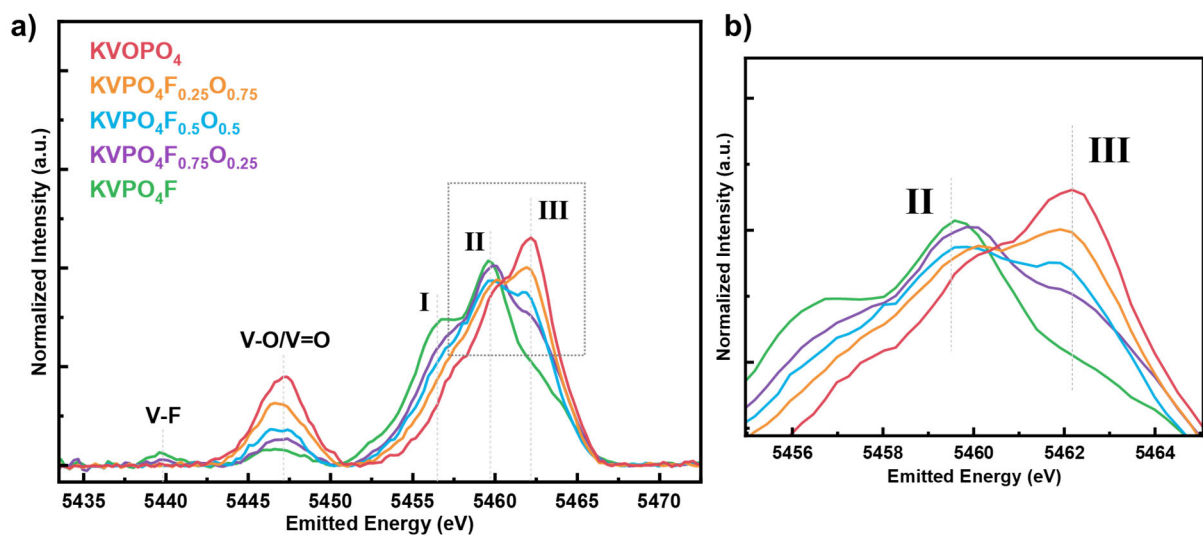


Figure S3. a) Normalized  $K\beta$  VtC XES emission lines of  $KVPO_4F_{1-x}O_x$  ( $x = 0, 0.25, 0.5, 0.75, 1$ ) and b) highlighted energy range where the isosbestic point of the five spectra lies.

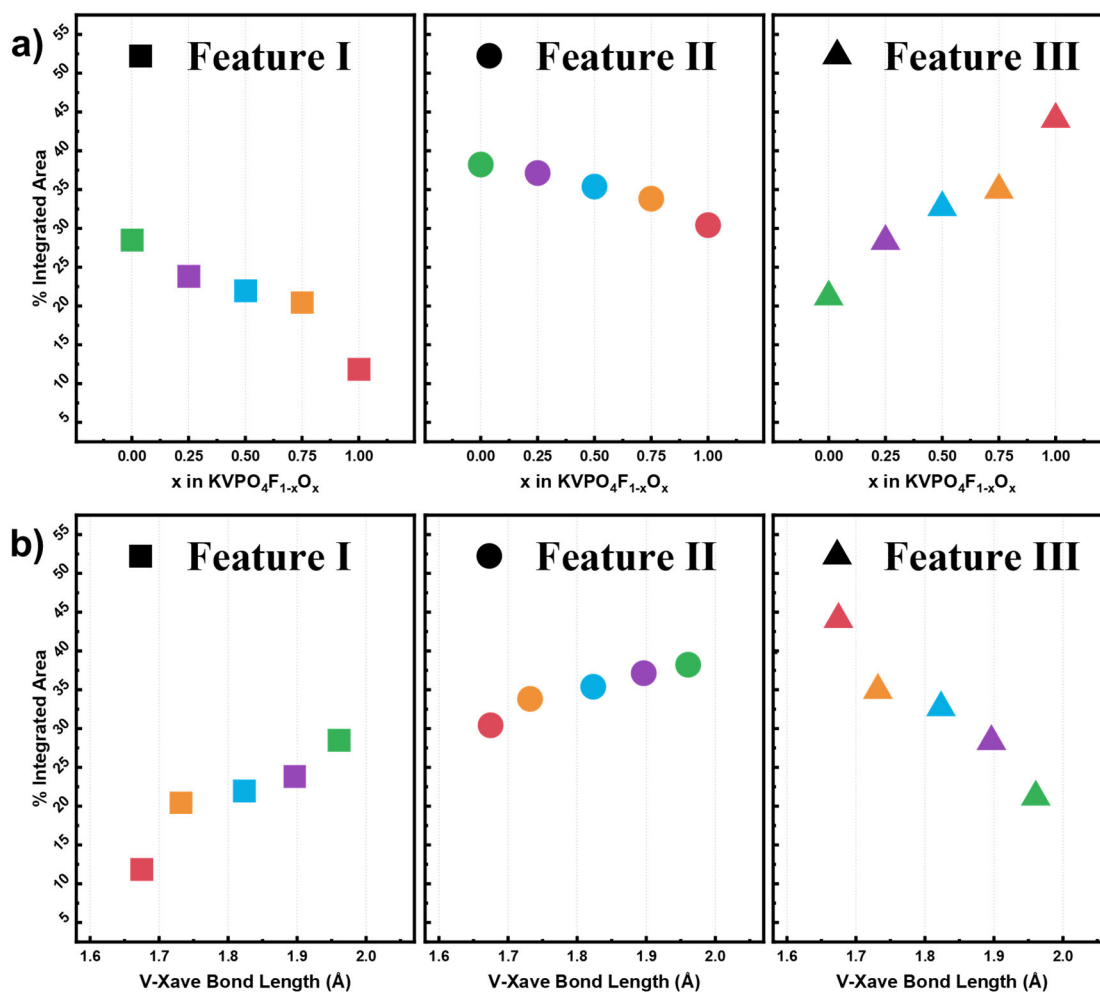


Figure S4. Graphical representation of the changes in the area of the contributions for features I, II, and III for the KVPO<sub>4</sub>F<sub>1-x</sub>O<sub>x</sub> series of materials: (a) correlation between composition  $x$  vs integrated area and (b) correlation between V-X<sub>ave</sub> bond length vs integrated area.

Table S4. Curve-fitting parameters and calculated contributions

<b>KVPO<sub>4</sub>F</b>	<b>Feature</b>	<b>Position, eV</b>	<b>FWHM</b>	<b>Area, %</b>	<b>Gaussian FWHM</b>	<b>Lorentzian FWHM</b>	<b>Weighted Sum of Squared Residuals</b>
V-O-P_O 2s*/2p	r <sub>i</sub>	5454.00	3.206	8.60	3.008	0.361	2.53 x 10 <sup>-6</sup>
V-O-P_O 2p	<b>I</b>	5456.61	2.848	28.52	2.672	0.321	
<b>V-F-V_F 2p, V-O-P_O 2p</b>	<b>II</b>	5459.57	2.764	<b>38.23</b>	<b>2.593</b>	<b>0.312</b>	
<b>V-O-P_O 2p</b>	<b>III</b>	5464.65	2.059	<b>21.18</b>	<b>1.932</b>	<b>0.232</b>	
V-O-P_O 2p	r <sub>ii</sub>	5462.31	3.262	3.48	3.060	0.368	
<b>KVPO<sub>4</sub>F<sub>0.75</sub>O<sub>0.25</sub></b>							
<b>KVPO<sub>4</sub>F<sub>0.75</sub>O<sub>0.25</sub></b>	<b>Feature</b>	<b>Position, eV</b>	<b>FWHM</b>	<b>Area, %</b>	<b>Gaussian FWHM</b>	<b>Lorentzian FWHM</b>	<b>Weighted Sum of Squared Residuals</b>
V-O-P_O 2s*/2p	r <sub>i</sub>	5454.39	2.873	5.58	2.695	0.324	1.83 x 10 <sup>-6</sup>
V-O-P_O 2p	<b>I</b>	5456.81	2.990	23.82	2.805	0.337	
<b>V-F-V_F 2p, V=O-V_O 2p σ/π</b>	<b>II</b>	5459.66	2.900	<b>37.14</b>	<b>2.721</b>	<b>0.327</b>	
<b>V=O-V_O 2p π</b>	<b>III</b>	5462.35	3.100	<b>28.34</b>	<b>2.909</b>	<b>0.349</b>	
V-O-P_O 2p	r <sub>ii</sub>	5464.36	2.265	5.12	2.125	0.255	
<b>KVPO<sub>4</sub>F<sub>0.5</sub>O<sub>0.5</sub></b>							
<b>KVPO<sub>4</sub>F<sub>0.5</sub>O<sub>0.5</sub></b>	<b>Feature</b>	<b>Position, eV</b>	<b>FWHM</b>	<b>Area, %</b>	<b>Gaussian FWHM</b>	<b>Lorentzian FWHM</b>	<b>Weighted Sum of Squared Residuals</b>
V-O-P_O 2s*/2p	r <sub>i</sub>	5454.60	2.822	5.76	2.648	0.318	1.69 x 10 <sup>-6</sup>
V-O-P_O 2p	<b>I</b>	5456.97	2.976	21.97	2.792	0.335	
<b>V-F-V_F 2p, V=O-V_O 2p σ/π</b>	<b>II</b>	5459.60	2.901	<b>35.39</b>	<b>2.722</b>	<b>0.327</b>	
<b>V=O-V_O 2p π</b>	<b>III</b>	5462.18	2.881	<b>32.69</b>	<b>2.703</b>	<b>0.325</b>	
V-O-P_O 2p	r <sub>ii</sub>	5464.32	2.165	4.19	2.031	0.244	
<b>KVPO<sub>4</sub>F<sub>0.25</sub>O<sub>0.75</sub></b>							
<b>KVPO<sub>4</sub>F<sub>0.25</sub>O<sub>0.75</sub></b>	<b>Feature</b>	<b>Position, eV</b>	<b>FWHM</b>	<b>Area, %</b>	<b>Gaussian FWHM</b>	<b>Lorentzian FWHM</b>	<b>Weighted Sum of Squared Residuals</b>
V-O-P_O 2s*/2p	r <sub>i</sub>	5454.98	2.920	5.45	2.740	0.329	1.09 x 10 <sup>-6</sup>
V-O-P_O 2p	<b>I</b>	5457.36	3.012	20.46	2.826	0.339	
<b>V-F-V_F 2p, V=O-V_O 2p σ/π</b>	<b>II</b>	5459.87	2.887	<b>33.83</b>	<b>2.709</b>	<b>0.325</b>	
<b>V=O-V_O 2p π</b>	<b>III</b>	5462.30	2.666	<b>34.94</b>	<b>2.501</b>	<b>0.300</b>	
V-O-P_O 2p	r <sub>ii</sub>	5464.39	1.858	5.32	1.744	0.209	
<b>KVOPO<sub>4</sub></b>							
<b>KVOPO<sub>4</sub></b>	<b>Feature</b>	<b>Position, eV</b>	<b>FWHM</b>	<b>Area, %</b>	<b>Gaussian FWHM</b>	<b>Lorentzian FWHM</b>	<b>Weighted Sum of Squared Residuals</b>
V-O-P_O 2s*/2p	r <sub>i</sub>	5455.97	3.183	6.90	2.987	0.359	1.53 x 10 <sup>-6</sup>
V-O-P_O 2p	<b>I</b>	5457.61	2.237	11.86	2.099	0.252	
<b>V=O-V_O 2p σ/π</b>	<b>II</b>	5459.89	2.602	<b>30.43</b>	<b>2.442</b>	<b>0.293</b>	
<b>V=O-V_O 2p π</b>	<b>III</b>	5462.31	2.633	<b>44.08</b>	<b>2.470</b>	<b>0.297</b>	
V-O-P_O 2p	r <sub>ii</sub>	5464.55	1.931	6.73	1.812	0.218	

\*r<sub>i</sub> and r<sub>ii</sub> are the residual contributions at the low emission energy and high emission energy, respectively, for the fitting procedure.



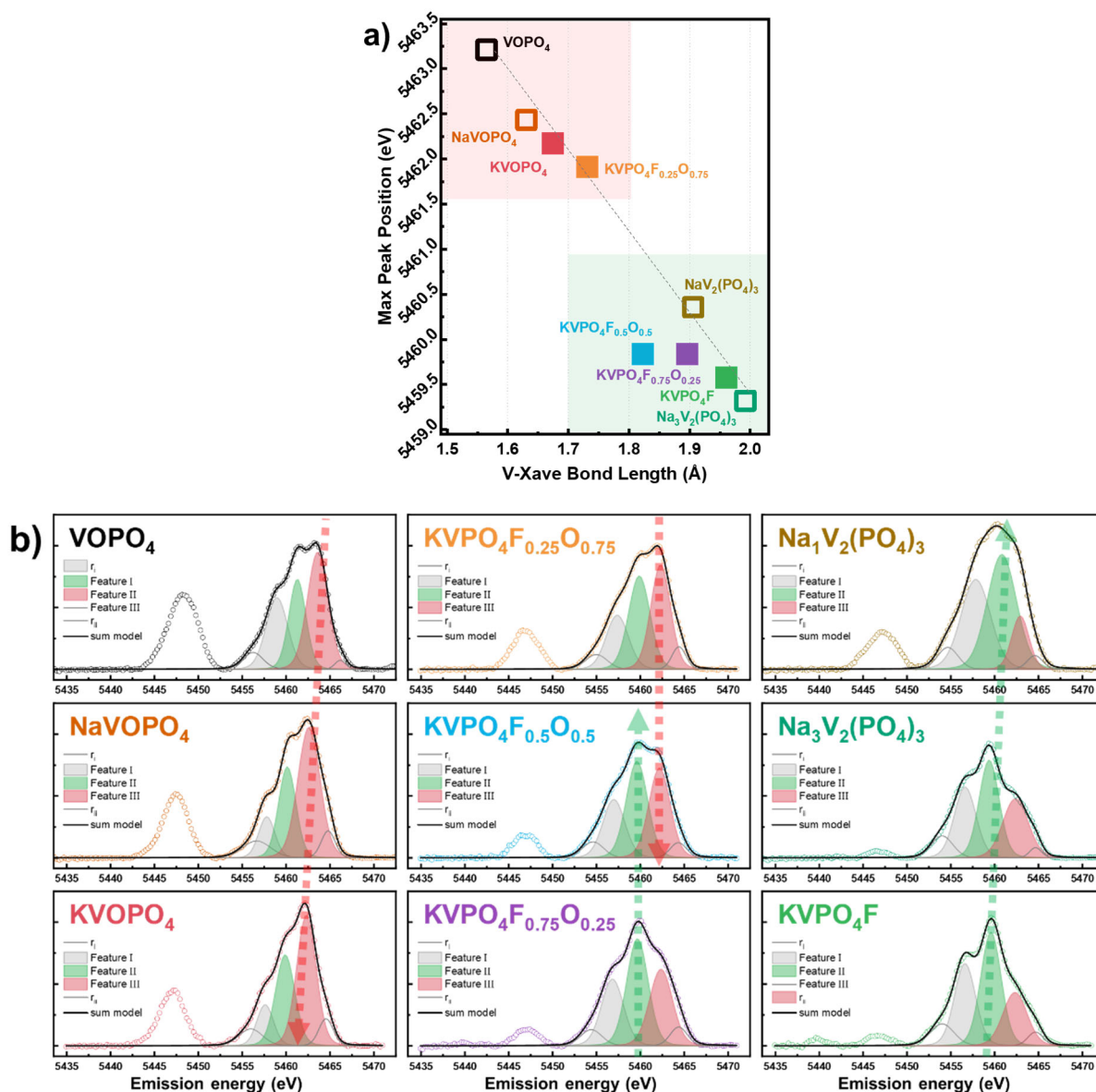
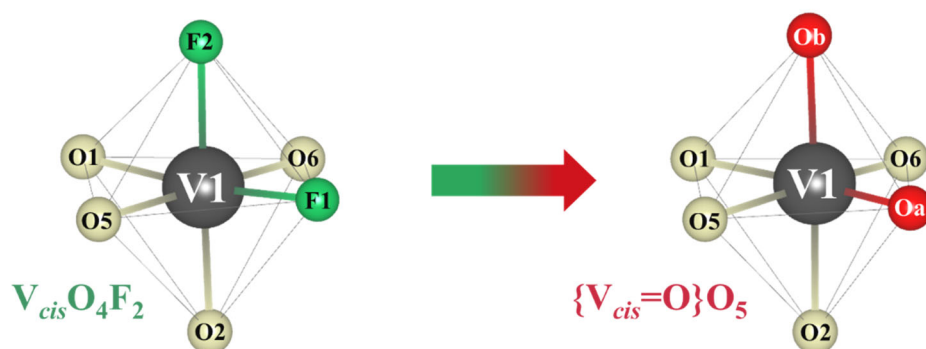


Figure S5. (a) The energy of the absolute maximum peak position of the VtC spectrum at the K $\beta_{2,5}$  region in relation to the average bond length of V=O for vanadyl containing compounds and average bond length of V-O for NaV<sub>2</sub>(PO<sub>4</sub>)<sub>3</sub> and Na<sub>3</sub>V<sub>2</sub>(PO<sub>4</sub>)<sub>3</sub> and (b) the experimental spectra of pristine and reference compounds along with the peak deconvolution using five Voigt functions

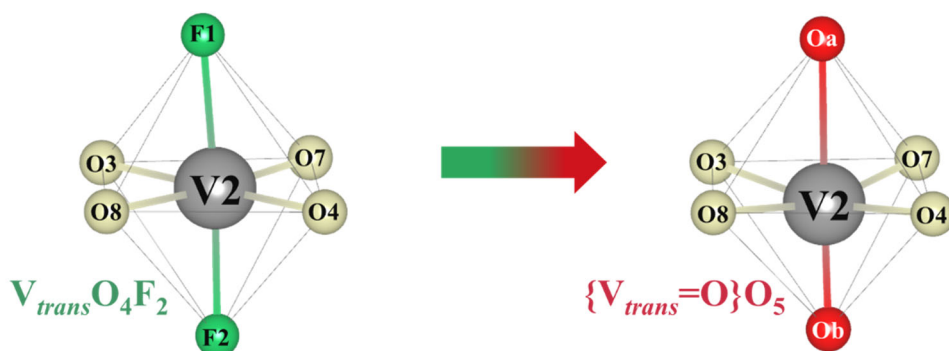
It should be noted that the intensities recorded at the maximum peak position (Feature II or Feature III, depending on the material) for the KVPO<sub>4</sub>F and KVOPO<sub>4</sub> end members exhibit a linear relationship with Na<sub>3</sub>V<sub>2</sub>(PO<sub>4</sub>)<sub>3</sub>, NaV<sub>2</sub>(PO<sub>4</sub>)<sub>3</sub>, NaVOPO<sub>4</sub>, and VOPO<sub>4</sub> reference materials concerning the average V-X bond lengths, indicating a high correlation between these parameters. However, no linear evolution is observed for compounds with partial compositions in the KVPO<sub>4</sub>F<sub>1-x</sub>O<sub>x</sub> series, especially KVPO<sub>4</sub>F<sub>0.5</sub>O<sub>0.5</sub>, which appears as an outlier in the trend mainly due to its mixed nature.

Additionally, a hypothesis can be formulated regarding the general disparity between ionicity and covalency concerning the presence of V-F and V=O bonds, particularly when considering features I and II (mainly feature II) in comparison with feature III. As depicted in Figure S5b, the deconvolution of all compounds (including references and pristine mixed materials) reveals feature III shaded in red, indicating a higher covalent environment, with an arrow pointing downward to signify decreasing covalency (from shorter to longer V=O bond lengths, from VOPO<sub>4</sub> to KVOPO<sub>4</sub> to KVPO<sub>4</sub>F<sub>0.5</sub>O<sub>0.5</sub>). Conversely, feature II is shaded in green, indicating a more ionic environment, with an arrow pointing upward towards a higher degree of covalency (from KVPO<sub>4</sub>F to NaV<sub>2</sub>(PO<sub>4</sub>)<sub>3</sub> to KVPO<sub>4</sub>F<sub>0.5</sub>O<sub>0.5</sub>).

Table S5. Bond lengths obtained from refined XRD patterns (Rietveld method) of the atoms around the (top) cis vanadium site and (bottom) trans vanadium site for  $\text{KVPO}_4\text{F}_{1-x}\text{O}_x$  ( $x = 0, 0.25, 0.5, 0.75, 1$ )<sup>2</sup>



$\text{V}_{cis}$	$\text{KVPO}_4\text{F}$	$\text{KVPO}_4\text{F}_{0.75}\text{O}_{0.25}$	$\text{KVPO}_4\text{F}_{0.5}\text{O}_{0.5}$	$\text{KVPO}_4\text{F}_{0.25}\text{O}_{0.75}$	$\text{KVOPO}_4$
V1-O1	1.961	1.964	1.964	1.981	1.994
V1-O2	1.928	1.944	1.972	1.978	1.985
V1-O5	2.032	2.046	2.029	2.033	2.008
V1-O6	1.979	1.993	1.979	1.977	1.994
V1-F1/=Oa	1.965	1.885	1.822	1.728	1.683
V1-F2/Ob	1.984	1.972	1.981	1.991	1.981



$\text{V}_{trans}$	$\text{KVPO}_4\text{F}$	$\text{KVPO}_4\text{F}_{0.75}\text{O}_{0.25}$	$\text{KVPO}_4\text{F}_{0.5}\text{O}_{0.5}$	$\text{KVPO}_4\text{F}_{0.25}\text{O}_{0.75}$	$\text{KVOPO}_4$
V2-O3	2.018	1.998	2.016	2.012	2.036
V2-O4	1.983	2.002	1.987	1.984	1.982
V2-O7	1.948	1.957	1.966	1.977	1.943
V2-O8	2.011	1.996	1.986	1.988	2.023
V2-F1/Oa	2.039	2.054	2.086	2.213	2.215
V2-F2/=Ob	1.957	1.908	1.825	1.735	1.666

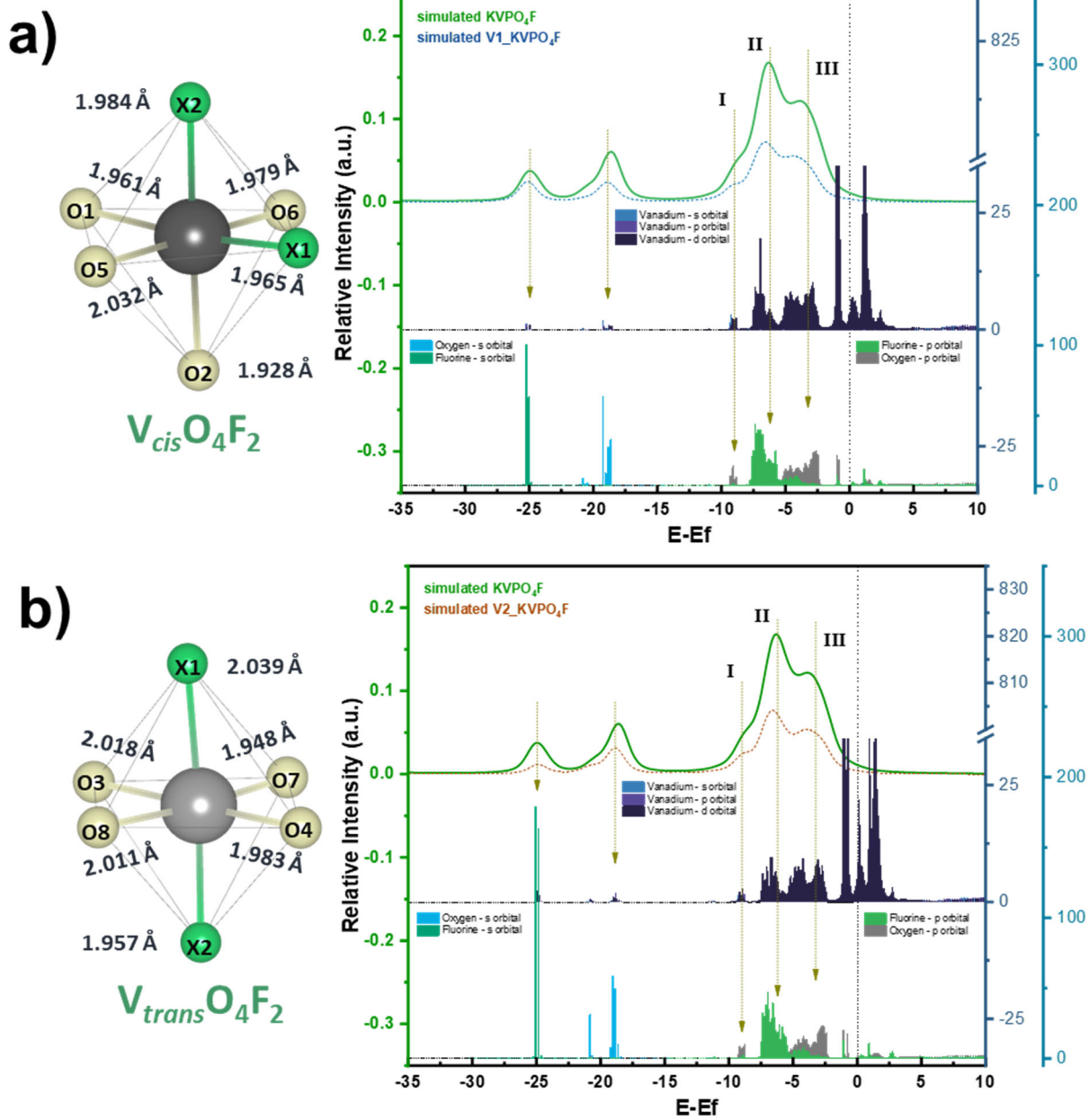


Figure S6. Calculated density of states for the simulated  $KVPO_4F$  spectra for a)  $V_{cis}O_4F_2$  and b)  $V_{trans}O_4F_2$

The density of states (DOS) obtained from the theoretical calculation performed can be deconvoluted to the individual contributions of the two different vanadium sites ( $V_{cis}$  and  $V_{trans}$ ) present in the material.<sup>2</sup> In  $KVPO_4F$ , it is noticeable that the features for both sites show similar characteristic which is related to the degree of bonding between V-O and V-F.

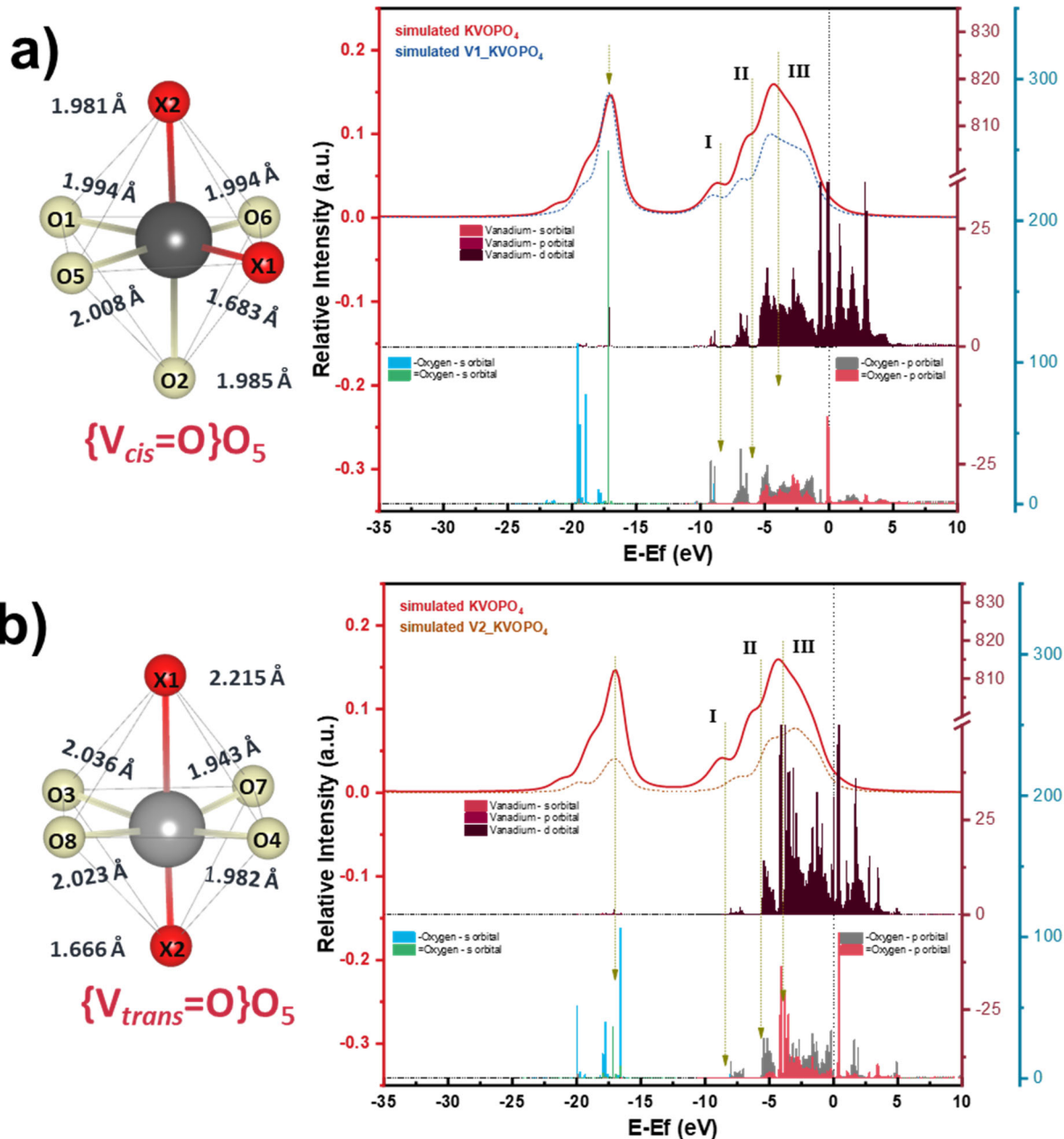


Figure S7. Calculated density of states for the simulated  $KVOPO_4$  spectra for a)  $\{V_{cis=O}\}O_5$  and b)  $\{V_{trans=O}\}O_5$

In contrast with  $KVPO_4F$ , a much bigger difference is observed for  $KVOPO_4$  especially at the  $K\beta_{2,5}$  region of both  $\{V_{cis=O}\}O_5$  and  $\{V_{trans=O}\}O_5$ . It can be deduced that due to the different position of the distortion causing vanadyl bonds, the hybridization of molecular orbitals varies and affects the overall electronic structure.

References:

- 1 E. Gallo and P. Glatzel, *Adv. Mater.*, 2014, **26**, 7730–7746.
- 2 R. Wernert, L. H. B. Nguyen, E. Petit, P. S. Camacho, A. Iadecola, A. Longo, F. Fauth, L. Stievano, L. Monconduit, D. Carlier and L. Croguennec, *Chem. Mater.*, 2022, **34**, 4523–4535.